# Sheath-Plasma Waves and Anomalous Loading in Ion-Bernstein-Wave Experiments

J. R. Myra and D. A. D'Ippolito
*Lodestar Research Corporation, Boulder, Colorado 80301*

D. W. Forslund and J. U. Brackbill
*Los Alamos National Laboratory, Los Alamos, New Mexico 87545*
(Received 31 August 1990)

It is proposed that the anomalous loading observed in tokamak ion-Bernstein-wave (IBW) experiments is due to a class of sheath-plasma waves (SPW) which propagate on high-voltage rf sheaths near the antenna. Particle simulations in one and two dimensions confirm the existence and scalings of the SPW. Coupling to the SPW modes can dominate coupling to the IBW, and qualitatively yields the observed dependences of antenna loading on parallel wave number, plasma density, and magnetic field. Antennas which minimize rf sheaths should improve the effectiveness of IBW heating.

PACS numbers: 52.40.Fd, 52.40.Hf, 52.50.Gj, 52.65.+z

A number of recent heating experiments in which ion Bernstein waves are launched into tokamaks show an anomalous resistive loading of the rf couplers.[1-5] The observed loading is several times larger than that predicted by standard coupling theory[6] and has different scalings with parallel wave number, frequency, magnetic field, and density. In this Letter we suggest an explanation for the observed anomaly: an additional class of waves near the antenna, sheath-plasma waves (SPW's), which propagate on the high-voltage rf sheaths driven by the antenna. We propose that the SPW carries away a portion of the launched power, giving rise to the observed anomalous loading.

Sheaths are an unavoidable consequence of material boundaries in all laboratory plasmas. At a sheath, the equilibrium gradients in the electron and ion densities allow a class of electrostatic surface waves, the SPW, to propagate along the sheath-plasma interface. The main results for unmagnetized plasmas[7,8] are as follows. A one-dimensional plasma of length $L$ bounded by static sheaths of width $\Delta/2$, treated here as vacuum layers, with a wave $(\omega,\mathbf{k})$ propagating along the sheaths has two normal modes. These have an electrostatic potential $\Phi$ of even and odd parity (see Fig. 1). For $k\Delta \ll 1$ one finds that $\omega \rightarrow \omega_{sp}$ $(\omega \rightarrow 0)$ for the odd- (even-) parity mode, where $\omega_{sp} \equiv \omega_{pe}(\Delta/L)^{1/2}$ is the series sheath-plasma resonance frequency identified in experiments by Stenzel[9] and $\omega_{pe} = (4\pi n_e e^2/m_e)^{1/2}$. For $k\Delta \gg 1$ both modes obey $\omega \rightarrow \omega_{pe}/\sqrt{2}$, as in the pioneering experiments on plasma column resonances.[7]

We now extend this eigenmode analysis to include the effect of a uniform magnetic field $\mathbf{B} = B\mathbf{b}$ and a tensor dielectric $\vec{\epsilon}$ in the plasma region. The geometry is shown in Fig. 1. Applying the boundary condition $\Phi = 0$ at the conducting boundaries and matching $\Phi$ and the normal component of electric displacement across the plasma interface yields the electrostatic dispersion relation (valid when $|\kappa_1 c| \gg \omega_{pi}$),

$$\frac{(p_1 \mathrm{th}_1 - k)(p_2 \mathrm{th}_2 + k)}{(p_1 \mathrm{th}_2 + k)(p_2 \mathrm{th}_1 - k)} = \exp(2\kappa_1 L), \qquad (1)$$

where $\mathrm{th}_1 = \tanh(k\Delta_1)$, $\mathrm{th}_2 = \tanh(k\Delta_2)$, $p_j = \kappa_j \epsilon_{ss} + ik\epsilon_{sk}$, $j = 1,2$. Here the components of the Hermitian tensor $\vec{\epsilon}$ are defined relative to $\mathbf{e}_s$ and $\mathbf{e}_k$ (see Fig. 1) and $\kappa_1 = -\kappa_2 = k(\epsilon_{kk}/\epsilon_{ss})^{1/2}$.

In the simple case of Fig. 1 with $\mathbf{B} \| \mathbf{e}_s$, Eq. (1) can be reduced to simpler forms depending on whether $\epsilon_\| \epsilon_\perp > 0$ (relevant to the *high-density* limit, $\omega_{pi} \gg \Omega_i = ZeB/m_i c$) or $\epsilon_\| \epsilon_\perp < 0$ (*low-density* limit, $\omega_{pi} \ll \Omega_i$) where $\epsilon_\| = \mathbf{b} \cdot \vec{\epsilon} \cdot \mathbf{b}$ and $\epsilon_\perp = \mathbf{e}_k \cdot \vec{\epsilon} \cdot \mathbf{e}_k$. The solutions of Eq. (1) in the high-density limit have been obtained numerically employing the hot-plasma Bessel-function expression for $\epsilon_\perp$, and are shown schematically in Fig. 2(a) for the case $\Omega_i < \omega < \omega_{\mathrm{lh}} < \omega_{pe}$. Here $\omega_{\mathrm{lh}} = [\Omega_i^2 + \omega_{pi}^2/(1 + \omega_{pe}^2/\Omega_e^2)]^{1/2}$ is the cold-fluid lower hybrid frequency. Coexisting with the ion-Bernstein-wave (IBW) modes (typical $k\rho_i \sim 1$), we find a branch of the SPW with typical $k\Delta \lesssim 1$ and *even parity*. The solutions in the low-density limit are shown schematically in Fig. 2(b) for the case $\Omega_i \lesssim \omega_{\mathrm{lh}} < \omega < \omega_{pe}$ and $k\rho_i \ll 1$. In this limit, the *odd-parity* SPW competes with the electron plasma wave (EPW). (In the conventional theory[10] the EPW

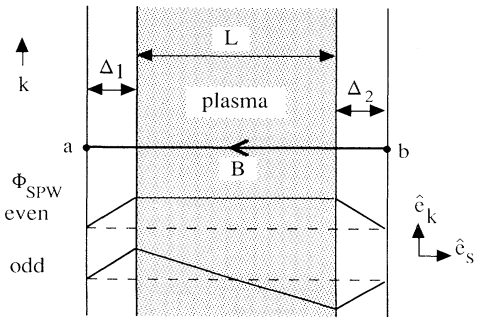


FIG. 1. Model geometry for the sheath-plasma-wave calculations showing a plasma of length $L$ bounded by sheaths of width $\Delta_1$ and $\Delta_2$. Waves propagate in the $\mathbf{e}_k$ direction. A magnetic-field line contacts conducting surfaces at points $a$ and $b$. Examples of the even- and odd-parity SPW modes are sketched.

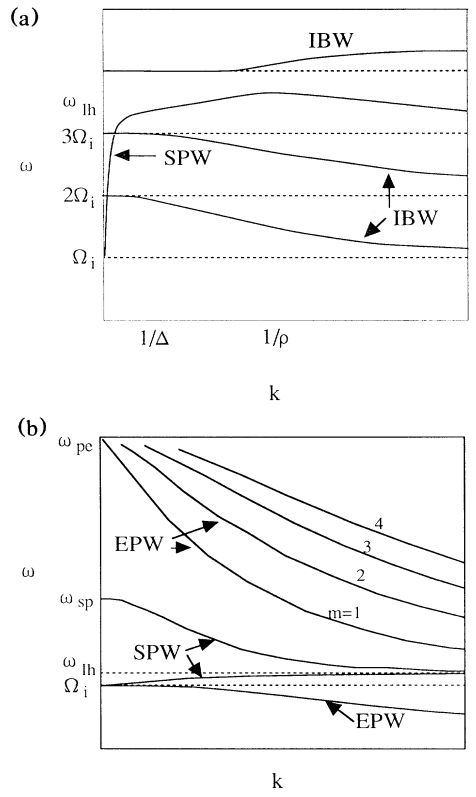


FIG. 2. Schematic representation of the dispersion relation for (a) the high-density and (b) the low-density regimes, showing the homogeneous plasma modes (IBW and EPW) and the SPW with (a) even parity and (b) odd parity. The $m$ numbers for the EPW correspond to quantized values of $k_\parallel$.

transforms to the IBW as the wave propagates towards the interior.)

For a given $\omega$ and density $n_a$ at the antenna, the coupling may be to both the desired IBW or EPW and the undesired SPW. The division of wave power between the competing modes must be obtained from wave-coupling calculations, the details of which will not be presented here. The analysis requires two assumptions: (i) small dissipation of the waves over a distance $2\pi/k$, and (ii) outgoing wave conditions (i.e., negligible reflection). For the SPW, this requires only that the waves propagate several wavelengths along the sheath-plasma interface. Qualitatively, one carries out a Laplace-transform analysis using separation of variables with separation constant $\Upsilon$, which plays the role of $k_\parallel$. Two situations must be distinguished. (i) In the high-$n_a$, hot-plasma case, two values of $k_\perp^2$ satisfy the dispersion relation for each $\Upsilon$ and $\omega$. The amplitudes of the excited IBW and SPW modes in the short-wavelength limit ($1/k_\perp <$ characteristic antenna dimension) are found from the Laplace-transform analysis to be $\Phi_{\rm IBW}=k_{\rm SPW}\Phi_a/(k_{\rm SPW}-k_{\rm IBW})$ and $\Phi_{\rm SPW}=k_{\rm IBW}\Phi_a/(k_{\rm IBW}-k_{\rm SPW})$, where $\Phi_a$ is the total amplitude at the antenna. Employing $k_{\rm IBW} \gg k_{\rm SPW}$ and the Poynting flux scaling for the power $P \propto k|\Phi|^2$ [see Eq. (3)], the ratio of power coupled into the two modes is

$$\frac{P(\mathrm{SPW})}{P(\mathrm{IBW})} \sim \frac{k_{\rm IBW}}{k_{\rm SPW}}, \tag{2}$$

i.e., the power couples preferentially to the mode whose wavelength is longest. Therefore, in the high-$n_a$ regime the even-parity SPW will typically carry away most of the launched power when $\Delta > \rho_i$. (Detailed analysis shows that a less restrictive inequality is usually sufficient to ensure $k_{\rm SPW} < k_{\rm IBW}$.) (ii) In the low-$n_a$, cold-plasma case, only one value of $k_\perp^2$ is obtained for each $\Upsilon$ and $\omega$. In this case, the SPW and the EPW will typically carry away a comparable amount of energy.

In our model the characteristic time-averaged sheath width $\Delta$ is that of the rf sheath driven by the applied rf voltage itself, given[11] by the Child-Langmuir law $\Delta = \lambda_{\rm De}(eV/T_e)^{3/4}$ where $V$ is the applied rf voltage and $\lambda_{\rm De}$ the Debye length. In high-power IBW experiments, antenna voltages are on the order of 10 keV resulting in large rf sheaths, $\Delta \gg \rho_i$. Then, it follows that the condition for efficient coupling to the SPW instead of the IBW is easily met. We argue that the existence of rf sheaths is a general feature of IBW antennas as for fast-wave antennas.[11,12] Where such sheaths form will depend on the particular geometry of the IBW antenna relative to the equilibrium magnetic-field lines. Possible field line contact points $a$ and $b$ of Fig. 1 are the Faraday screen, antenna side protection tiles, or adjacent plasma limiters. The geometry of Fig. 1 and the model based on it are too crude to make reliable quantitative predictions for most of these sheaths. Nonetheless, their existence will lead to SPW's, perhaps different in detail from those discussed here, but still competing with the IBW and EPW for wave power. This is the main conceptual point of our paper.

Because the preceding SPW model is highly idealized (e.g., sharp-boundary static sheath interface) it is important to investigate the robustness of our most important conclusion: the existence of the SPW branch for rf-driven sheaths in a magnetized plasma. To this end, we briefly present some results of fully kinetic 1D and 2D particle simulations. In fact, it was the unexpected observation of large SPW oscillations in the simulations which initially motivated the present work.

The simulation results which follow were obtained with the new variable-zoning code CELESTE.[13] In the simulation, two conducting plasma boundaries at $x=0$ and $L$ were oscillated at voltage $V=\pm V_0\sin(\omega t)\times\sin(ky)$, simulating odd-parity drive, where $y$ is the direction of wave propagation. Figure 3 shows the time history of the electric-field energy and its power spectrum for the parameters $L=100$, $\omega=0.01$, $m_i=100$, $B_x=3$, and $eV/T_e=10$ (in units where $\omega_{pe}=e=m_e=c=1$). The SPW frequency, which lies between $5\omega$ and $6\omega$ for these parameters, is clearly evident.[14] A

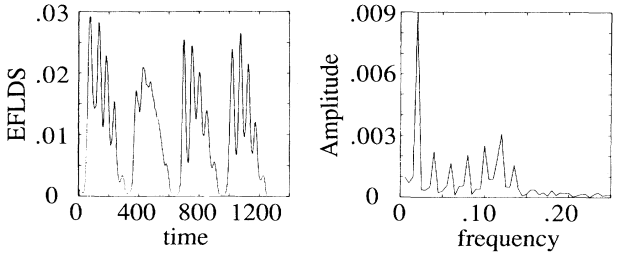


FIG. 3. Time history of the electric-field energy and the power spectrum for a 1D particle simulation of an rf-driven sheath. The SPW frequency lies between 5 and 6 times the rf drive frequency.

number of simulations similar to that of Fig. 3, and summarized in Table I, have enabled verification of the analytically predicted scalings of the SPW frequency with system length $L$, applied voltage $V$, and wave number $k$. Table I shows that the sharp-boundary analytical sheath model presented here adequately describes the qualitative features of the SPW branch, and positively identifies the oscillations seen in the simulations.

When the SPW is the dominant wave loading an antenna, it is possible to obtain an estimate of the expected loading resistance and its scalings under the same assumptions discussed before Eq. (2). Following the method of Bers,[15] the launched power may then be related to the wave potential $\Phi$ by

$$P=-\int \frac{dA}{16\pi}|\Phi|^2\omega\frac{\partial}{\partial k}(k^2\epsilon_\perp)\,, \tag{3}$$

where $dA$ is an area element with unit normal in the direction of $\mathbf{e}_k$. For definiteness we consider side-protection-tile sheaths and take the $\mathbf{e}_k$ direction to be radial. In order of magnitude, we employ $\int dA\sim A$, $P\sim|\Phi|^2R/2Z^2$, where $A$ is the antenna area and $Z=|\Phi/I|$ is an impedance. For IBW loop couplers the impedance is dominantly inductive and $Z\sim\omega L_a$ with $L_a$ the inductance of the strap carrying current $I$. Making these substitutions, Eq. (3) implies a scaling for the loading resistance $R$ given by

$$R\sim AZ^2\omega k_{\mathrm{SPW}}\epsilon_\perp/4\pi\,. \tag{4}$$

It is interesting to compare the predicted dependence of $R$ with the DIII-D data of Ref. 1. We find qualitative agreement with four features: order of magnitude, phasing dependence, density scaling, and $B$ field dependence. (i) Order of magnitude: Reasonable choices of $A$ (2000 cm$^2$) and rf sheath voltage (2 kV) yield $R$ in the range 1–10 $\Omega$, as measured. (ii) Phasing dependence: In the high- (low-) $n_a$ limit, $\Phi_{\mathrm{SPW}}$ has even- (odd-) parity and our model predicts that $R$ will be largest for an antenna phasing that favors an even- (odd-) parity rf voltage. This corresponds to odd- (even-) parity antenna current and high- (low-) $k_\parallel$ phasing. The theory predicts that the parity and phasing for maximum loading change at a critical density $n_{\mathrm{lh}}$ is given by $\omega=\omega_{\mathrm{lh}}$. Experimentally, it has been found that at high (low) density, $R$ is maximized for high- (low-) $k_\parallel$ phasing, referred to here as the "dominant" phasing. (iii) Density scaling: Measurements[1] of $R$ vs $n_a$ (antenna-plasma separation) for the dominant phasing show that $R$ is large and increases with density in the high-$n_a$ regime; $R$ is smaller and less sensitive to density in the low-$n_a$ regime. Numerical solutions show that the theoretical density scaling of $R\propto k_{\mathrm{SPW}}\epsilon_\perp$ is qualitatively that of $|\epsilon_\perp|=|1-n_a/n_{\mathrm{lh}}|$ which reproduces both features of the data and suggests a transition at $n_a=n_{\mathrm{lh}}$. (iv) $B$ field dependence: Equation (4) predicts that $R$ is approximately independent of $B$ except near $\omega=\Omega_i$. In particular, $R$ shows no resonantlike features at $\omega=2\Omega_i$ in contrast with conventionally predicted IBW loadings.[6] Experimentally, the observed dependence on $B$ is weak for $\omega>\Omega_i$, with no observable resonance at $\omega=2\Omega_i$. The preceding features, insofar as they have been measured, typify the observed anomalous loading in a number of experiments.[1-5]

TABLE I. Comparison of particle simulation and theory for the scaling of the SPW frequency with system $L$ (cases 1, 2, and 3), driving voltage $V$ (cases 4, 1, and 5), and wave number $k$ (cases 6 and 7).

| Case | $L/\lambda_{De}$ | $eV/T_e$ | $k\lambda_{De}$ | $\omega_{SPW}$ simulation | $\omega_{SPW}$ theory |
|---|---|---|---|---|---|
| 1 | 250 | 10 | 0 | 0.10 | 0.12 |
| 2 | 1000 | 10 | 0 | 0.05 | 0.06 |
| 3 | 4000 | 10 | 0 | 0.02 | 0.03 |
| 4 | 250 | 5 | 0 | 0.08 | 0.09 |
| 1 | 250 | 10 | 0 | 0.10 | 0.12 |
| 5 | 250 | 20 | 0 | 0.12 | 0.15 |
| 6 | 1000 | 10 | 0 | 0.05 | 0.06 |
| 7 | 1000 | 10 | 0.05 | 0.04 | 0.05[a] |

[a]Sheath width for this estimate is based on the $y$-averaged driving voltage $\approx V_0/\pi$.

These results suggest that rf sheaths and associated sheath waves are the key to understanding anomalous loading in IBW experiments. If this hypothesis is verified, there are at least two strategies for improving the prospects for IBW heating of tokamak plasmas. First, the relative power drain by the SPW branch is least severe in the low-density limit, a fact which favors the EPW launch scheme[10] over direct high-density IBW launch. Second, there is the more general avenue of designing antennas (or waveguide couplers) which minimize the formation of high-voltage rf sheaths altogether. These sheaths arise whenever there is rf flux linkage through a circuit consisting of the launch structure and magnetic-field lines which intersect its surfaces. Techniques for minimizing this flux linkage, which rely on geometrical and phasing symmetries and $B$-field–antenna alignment, have already proven their usefulness in reducing impurity production at the Faraday screen of

fast-wave antennas.[12] Extension of these sheath-control concepts from the fast-wave to the IBW context will be an interesting and important area for future experimental and theoretical investigations.

The authors wish to thank R. E. Aamodt, P. J. Catto, T. Intrator, M. J. Mayberry, and R. I. Pinsker for beneficial discussions. This work was supported by the U.S. Department of Energy.

[1]R. I. Pinsker, M. J. Mayberry, M. Porkolab, and R. Prater, in *Proceedings of the Eighth Topical Conference on Applications of Radio-Frequency Power to Plasmas, Irvine, California, 1989* (AIP, New York, 1989); R. I. Pinsker *et al.*, Bull. Am. Phys. Soc. **34**, 2120 (1989); (private communication).

[2]Y. Takase *et al.*, Phys. Rev. Lett. **59**, 1201 (1987).

[3]M. Ono *et al.*, Phys. Rev. Lett. **60**, 294 (1988); (private communication).

[4]R. Koch *et al.*, Fusion Eng. Des. **12**, 15 (1990).

[5]S. Shinohara, O. Naito, and K. Miyamoto, J. Phys. Soc. Jpn. **57**, 665 (1988).

[6]M. Brambilla, Nucl. Fusion **28**, 549 (1988).

[7]N. A. Krall and A. W. Trivelpiece, *Principles of Plasma Physics* (McGraw-Hill, New York, 1973), pp. 157–167, and references therein.

[8]G. Bekefi, *Radiation Processes in Plasmas* (Wiley, New York, 1966), pp. 168–173.

[9]R. L. Stenzel, Phys. Rev. Lett. **60**, 704 (1988); Phys. Fluids B **1**, 2273 (1989).

[10]M. Ono, K. L. Wong, and G. A. Wurden, Phys. Fluids **26**, 298 (1983).

[11]J. R. Myra, D. A. D'Ippolito, and M. J. Gerver, Nucl. Fusion **30**, 845 (1990); F. W. Perkins, Nucl. Fusion **29**, 583 (1989).

[12]D. A. D'Ippolito, J. R. Myra, M. Bures, and J. Jacquinot, Lodestar Research Corporation Report No. LRC-90-18, 1990 (unpublished); M. Bures *et al.*, JET Report No. JET-P(90)49, 1990 (unpublished).

[13]J. U. Brackbill *et al.*, Bull. Am. Phys. Soc. **35**, 2003 (1990).

[14]The mechanism which feeds energy into the SPW in these simulations, enabling their identification, is discussed in R. Stenzel, H. C. Kim, and A. Y. Wong, Radio Sci. **10**, 485 (1974).

[15]A. Bers, in *Plasma Physics,* Les Houches Summer School of Theoretical Physics, edited by C. DeWitt and J. Peyraud (Gordon & Breach, New York, 1975), pp. 126–137.